

# Can tidal tomography be used to unravel the long-wavelength structure of the lunar interior?

Shijie Zhong,<sup>1</sup> Chuan Qin,<sup>1</sup> Geruo A,<sup>1</sup> and John Wahr<sup>1</sup>

Received 14 May 2012; revised 9 July 2012; accepted 11 July 2012; published 15 August 2012.

[1] The Moon displays a number of hemispherically asymmetric features that may be related to long-wavelength structure and dynamics in the lunar mantle. Here we propose to use observations of the non-degree-2 gravitational response of the Moon to degree-2 tidal forcing to constrain the long-wavelength lunar mantle structure. For a planetary body with laterally varying structure, degree-2 tidal forces excite gravitational response at non-degree-2 harmonics due to mode coupling effects. Using a new numerical model, we determine that for a lunar mantle with  $\sim 5\%$  hemispherical variations in seismic shear wave velocity  $V_s$ , the degree-3 response could reach  $\sim 2\%$  of the degree-2 response. The larger the hemispherical variations in  $V_s$ , the larger the degree-3 response. We suggest that if observations from recent lunar missions such as SELENA and GRAIL could be used to determine the non-degree-2 tidal response, it might be possible to place constraints on the lunar mantle structure. **Citation:** Zhong, S., C. Qin, G. A., and J. Wahr (2012), Can tidal tomography be used to unravel the long-wavelength structure of the lunar interior?, *Geophys. Res. Lett.*, 39, L15201, doi:10.1029/2012GL052362.

## 1. Introduction

[2] The Moon displays a number of hemispherically asymmetric features. First, the nearside topography is several kilometers lower than the farside [Zuber *et al.*, 1994], which is often interpreted as the consequence of a thicker crust on the farside than on the nearside [Neumann *et al.*, 1996]. Second, there is a high surface concentration of radioactive elements in the Procellarum KREEP terrane (PKT) on the nearside [Lawrence *et al.*, 2002]. Third, mare basalts, as the most important volcanic event in lunar geological history, erupted predominantly on the nearside from  $\sim 3.9$  Ga to  $\sim 3$  Ga [e.g., Wieczorek *et al.*, 2006]. Fourth, deep moonquakes (DMQ) are mostly located on the nearside at depths of  $\sim 800$  km, although the nearside distribution of DMQ may result from a biased distribution of Apollo seismic stations and/or large attenuation in the mantle that make it hard to detect DMQ on the farside [e.g., Nakamura, 2005].

[3] A number of studies over the last three decades have explored physical mechanisms for forming these hemispherically asymmetric features and their relationships. Crustal production and mare basalt volcanism may reflect

the thermochemical structure and dynamics of the early lunar mantle. That is, the early mantle may have been dominated by hemispherically asymmetric structure, responsible for the global asymmetries in crustal thickness and mare basalt distribution [Zhong *et al.*, 2000; Parmentier *et al.*, 2002; Wieczorek and Phillips, 2000; Wieczorek *et al.*, 2006; Garrick-Bethell *et al.*, 2010]. DMQs reveal present-day deformation of the lunar mantle. Although DMQs are closely related to tidal forces [e.g., Lammlein, 1977], mantle structure, including heterogeneities and the distribution of volatiles, could also play important roles in determining the DMQ spatial pattern [Frohlich and Nakamura, 2009]. Recently, statistical analysis has suggested that DMQs correlate with the mare basalt distribution [Qin *et al.*, 2012]. This leads to the hypothesis that DMQs may delineate the volatile-rich mare basalt source region in the present-day lunar mantle, which still retains its early hemispherically asymmetric structure and that may have been responsible for mare basalt genesis [Qin *et al.*, 2012].

[4] While future seismic tomography could provide a straightforward test of Qin *et al.*'s [2012] hypothesis, we propose here that tidal tomography using satellite gravity observations of the tidal response of the Moon from recent lunar missions, could provide a preliminary evaluation. The rationale is that when subject to degree-2 tidal forcing, a planetary body with laterally varying elastic structure will exhibit a characteristic non-degree-2 response that is sensitive to the pattern and amplitude of the lateral variability [e.g., Latychev *et al.*, 2009]. In this study, we determine the non-degree-2 tidal response of the Moon with a hemispherically asymmetric mantle structure, and explore the possibility of using observations of the tidal response to test Qin *et al.*'s [2012] hypothesis concerning present-day lunar mantle structure.

## 2. Physical Model and Methods

[5] We model the Moon as a compressible, self-gravitating, and elastic solid that deforms in response to an applied tidal force. The governing equations are given in Wahr *et al.* [2009], and for an unperturbed density distribution  $\rho_0$  that is radially symmetric, are briefly summarized as follows.

$$\sigma_{ij,j} + \rho_0 \varphi_{,i} - \rho_1^E g_i - (\rho_0 g u_r)_{,i} + \rho_0 V_{T,i} = 0 \quad (1)$$

$$\varphi_{,ii} = -4\pi G \rho_1^E, \quad (2)$$

where  $\rho_1^E = -(\rho_0 u_i)_{,i}$  is the Eulerian density perturbation,  $u_i$  is the  $i$ 'th component of the displacement,  $u_r$  is the radial displacement,  $\sigma_{ij}$  is the stress tensor,  $g_i$  is the  $i$ 'th component of the unperturbed gravitational acceleration,  $\varphi$  is the perturbation to the lunar gravitational potential,  $V_T$  is the tidal

<sup>1</sup>Department of Physics, University of Colorado at Boulder, Boulder, Colorado, USA.

Corresponding author: S. Zhong, Department of Physics, University of Colorado at Boulder, Boulder, CO 80309, USA. (szhong@colorado.edu)

**Table 1.** Model Parameters and Constants<sup>a</sup>

Depths (km)	$\rho_0$ (kg/m <sup>3</sup> )	$V_p$ (km/s)	$V_s$ (km/s)
0–15	2700	3.2	1.8
15–40	2800	5.5	3.2
40–238	3300	7.7	4.4
238–488	3400	7.8	4.4
488–738	3400	7.6	4.4
738–1257	3400	8.5	4.5
1257–1407	3400	7.5	3.2
1407–1497	5100	–	–
1497–1740	8000	–	–
Semi-major axis, $a$		$3.844 \times 10^8$ m	
Eccentricity, $\epsilon$		0.0549	
Earth's mass, $m$		$5.97 \times 10^{24}$ kg	
Moon's radius, $R_s$		$1.74 \times 10^6$ m	

<sup>a</sup>The model of the density and seismic velocities is from *Weber et al.* [2011].

potential,  $G$  is the gravitational constant, and the notation  $A_{,i}$  represents the derivative of the variable  $A$  with respect to  $x_i$ .  $\sigma_{ij}$  can be related to the displacement field as

$$\sigma_{ij} = \lambda u_{i,i} + \mu(u_{i,j} + u_{j,i}), \quad (3)$$

where  $\lambda$  is the Lamé parameter and  $\mu$  is the shear modulus.

[6] The time-dependent components of the tidal potential,  $V_T$ , are [*Kaula, 1964; Wahr et al., 2009*]

$$V_T(r, \theta, \phi, t) = \frac{3\epsilon GmR_S^2}{4a^3} \left(\frac{r}{R_S}\right)^2 \left\{ [(1 - 3\cos^2\theta) + 3\sin^2\theta \cos(2\phi)] \cos(nt) + 4\sin^2\theta \sin(2\phi) \sin(nt) \right\}, \quad (4)$$

where  $t$  is the time;  $r$ ,  $\theta$ , and  $\phi$  are the radius, co-latitude, and longitude (measured eastward from the sub-Earth point);  $R_S$  is the Moon's radius;  $a$  and  $\epsilon$  are the semi-major axis and eccentricity of the lunar orbit;  $m$  is the Earth's mass; and the mean motion  $n$  is  $2\pi/T$  where  $T$  is the orbital period which, since the Moon's rotation is synchronous with its orbital motion, is also equal to its angular velocity of rotation. The  $\cos(nt)$  term in (4) represents forcing caused by time-dependent variations in the Earth-Moon distance for an eccentric orbit (i.e., radial tidal forcing), and the  $\sin(nt)$  term describes librational tidal forcing [*Wahr et al., 2009*]. Parameter values are given in Table 1. Note that the radial tidal forcing has two distinct spherical harmonics: one at (2, 0) (we use notation ( $l, m$ ) to represent degree  $l$  order  $m$  throughout the paper), and the other at (2, 2) (i.e., the first and second terms, respectively, in the  $\cos(nt)$  bracket (4)), while the librational tidal forcing includes only a (2, 2) harmonic. For simplicity, we consider only the radial tidal forcing in this study. The librational tide with  $\sin(nt)$  time dependence has a different phase from the radial tide, and in principle these two tides can be separated.

[7] The response of a spherically symmetric planetary body (i.e., where the density and elastic parameters  $\lambda$  and  $\mu$  only depend only on the radius  $r$ ) to the tidal potential (4) is characterized by the same degree 2 harmonics that are present in that potential, but with a more complicated radial dependence. That radial dependence is traditionally determined by solving equations (1) and (2) subject to continuity conditions across internal boundaries and the outer surface [e.g., *Tobie et al., 2005; Wahr et al., 2009*]. The response at

the surface is usually expressed in terms of Love numbers  $h_2$  and  $k_2$ , for the radial displacement and gravitational potential, respectively. However, when lateral variability (i.e., 3-D elastic structures) is present, the tidal response no longer occurs only at  $l = 2$ , Non-degree 2 displacement and gravity signals emerge, with amplitudes that depend on the wavelengths and amplitudes of the lateral variations in elastic structures.

[8] To solve (1) and (2) for a planetary body with 3-D elastic structures, one must rely on numerical methods [*Zhong et al., 2003; Paulson et al., 2005; Latychev et al., 2009*]. In this study, we use a modified finite element code CitcomSVE to compute the response. CitcomSVE was originally developed for solving post-glacial rebound problems for a 3-D incompressible, viscoelastic Earth [*Zhong et al., 2003; Paulson et al., 2005*]. Recently, this code has been modified for compressible media, and the modifications will be described in a separate paper. For this study, we use the code to solve (1) and (2) and to determine the tidal response for a lunar mantle with a hemispherically asymmetric (i.e., degree-1) elastic structure. We do not consider viscoelastic effects, which we expect to be of secondary importance for tidal deformation at monthly time scales.

[9] We use a recently published 1-D model of S-wave speeds, P-wave speeds and density for the Moon as the 1-D background (Table 1) [*Weber et al., 2011*]. A hemispherically asymmetric (i.e., degree-1) elastic structure is introduced as a relative shear wave seismic velocity variation (note  $V_S = \sqrt{\mu/\rho_0}$ )

$$dV_S/V_S = -\Delta \sin \theta \cos \phi, \quad (5)$$

that is added to the S-wave speed  $V_S$  at all depths, where  $\Delta$  is an arbitrary amplitude and is independent of depth. Equation (5) represents a (1, 1) variation where for positive  $\Delta$  the nearside has a slower seismic velocity than the farside. We assume, for simplicity, that the lateral variations in  $V_S$  occur only in the shear modulus  $\mu$ , and that neither the density  $\rho_0$  nor the Lamé parameter  $\lambda$  contains lateral variations. We assume that  $\Delta$  varies from 1.25% to 15% in this study, but a more reasonable upper limit for variations is probably 5–10%. The pressure at the lunar core-mantle boundary is similar to that at  $\sim 200$  km depth in the Earth, which is near the bottom of the continental lithosphere.  $V_S$  may vary by 10% laterally over this depth range in the Earth [e.g., *Ritsema et al., 1999*].

### 3. Results

[10] We first demonstrate the accuracy of our finite element code CitcomSVE for solving tidal forcing problems, by comparing the degree-2 response of a spherically symmetric Moon (i.e., the Love numbers  $k_2$  and  $h_2$ ) determined from the code with those computed using the traditional solution method [e.g., *Wahr et al., 2009*]. The Love numbers  $k_2$  and  $h_2$  depend only on the planetary density and elastic structure and are independent of tidal amplitude [e.g., *Lambeck, 1980*]. For the Moon with the 1-D structure of *Weber et al.* [2011] (Table 1),  $k_2$  and  $h_2$  from the traditional solutions are 0.023410 and 0.040933, respectively, which are consistent with the results of *Weber et al.* [2011] and *Konopliv et al.* [2001].

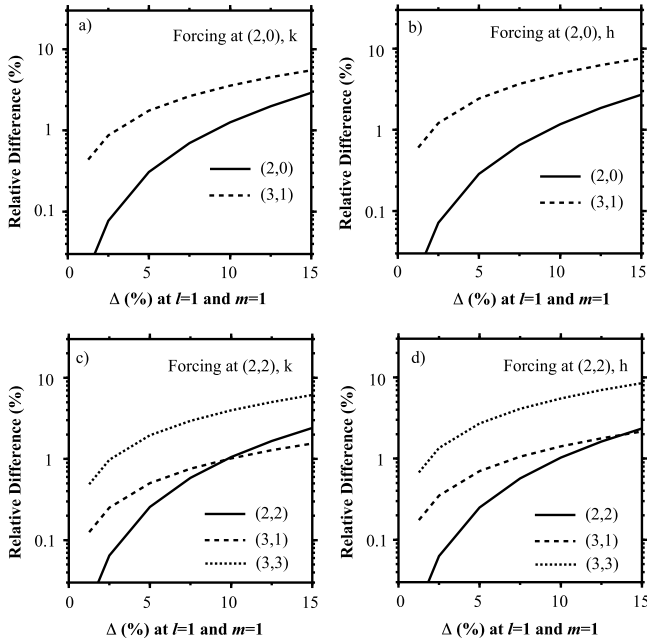


**Figure 1.** Relative differences in the tidal response at degrees 2 and 3 versus the amplitude of degree-1 variations in S-wave speed,  $\Delta$ , for (a) gravitational potential and (b) radial displacement for  $l = 2$   $m = 0$  tidal forcing; (c and d) for  $l = 2$   $m = 2$  tidal forcing. The relative difference for the response at harmonic degree  $l$  order  $m$  is defined as  $|X_{lm} - X_{lm}^0|/X_{lm}^0$ , where  $X_{lm}$  is the gravitational potential or radial displacement response using the spherical harmonic functions defined in *Zhong et al.* [2008],  $X_{lm}^0$  is the response at the degree-2 forcing harmonic, and the superscript 0 represents the results from a case with no lateral variations in structure. Note that the response at the (3,3) harmonic is not presented in Figures 1a and 1b, but is about 2 orders of magnitude smaller than that at the (3,1) harmonic.

[11] We compute  $k_2$  and  $h_2$  using CitcomSVE on three different sets of grids:  $12 \times 48^3$ ,  $12 \times 64^3$ , and  $12 \times 80^3$ , which correspond to a total of  $1.3 \times 10^6$ ,  $3.1 \times 10^6$ , and  $6.1 \times 10^6$  elements, respectively. In the CitcomS code, the spherical mantle is divided into 12 approximately equal size caps, and each cap is further discretized into  $p$  cells in each of the two horizontal directions and  $q$  cells in the radial direction. The total number of elements is therefore  $12p^2q$  [e.g., *Zhong et al.*, 2008]. For the  $12 \times 48^3$  grid, using a (2, 0) tidal potential,  $k_2$  and  $h_2$  are 0.023396 and 0.040894, respectively, which differ from the traditional solution by 0.06% and 0.1%, respectively. There are non-zero responses at non-degree 2 harmonics due to numerical errors, but they are typically 4 orders of magnitude smaller than the degree 2 component. The numerical errors decrease with increasing resolution. For the  $12 \times 80^3$  grid, our numerical solutions are  $k_2 = 0.023417$  and  $h_2 = 0.040921$ , representing errors of 0.03% and 0.025%, respectively. We also compute the Love numbers using a (2, 2) tidal potential, and they differ only slightly from those computed for the (2, 0) tidal potential, as expected. We use the  $12 \times 80^3$  grid for all the following calculations.

[12] We next compute the response of a Moon that includes the degree-1 shear moduli variations given in (5). Because of mode coupling caused by lateral variation, we expect

responses at other harmonics in addition to degree 2 [e.g., *Dahlen and Tromp*, 1998]. When only the (2, 0) tidal potential is applied, the largest non-degree 2 response in the gravitational potential and radial displacement occurs at (3, 1) and is  $\sim 2\%$  of the  $l = 2$  response when the degree-1 variation in  $dV_s/V_s$  is 5% (i.e.,  $\Delta = 5\%$ ) (Figures 1a and 1b). The  $l = 3$  response increases with the value of  $\Delta$  in a non-linear fashion. The lateral variations also cause the  $l = 2$  response (i.e., the Love numbers) to change, but the relative change is  $< 1\%$  unless  $\Delta \sim 10\%$  or larger. For a (2, 2) tidal potential, the largest non-degree 2 response occurs at (3, 3), although the response at (3, 1) is also significant (Figures 1c and 1d). Similarly, the response at (3, 3) is  $> 2\%$  of the  $l = 2$  response for  $\Delta \sim 5\%$ .

[13] Using the complete tidal potential for radial tidal forcing (i.e., the  $\cos(nt)$  term in (4)) that contains both the  $m = 0$  and  $m = 2$  terms, we compute the response of a Moon in which the degree-1 variation in  $dV_s/V_s$  is 7.5% (i.e.,  $\Delta = 7.5\%$ ), and show a map of the results in Figures 2a and 2b. Those figures show the radial tide's full amplitude (i.e., the response at  $t = 0$ ). The gravitational and radial displacement responses are dominated by the harmonics of the forcing (i.e., (2, 0) and (2, 2)) (Figure 2a), but the difference from the results determined for a spherically symmetric model (i.e., for  $\Delta = 0$ ) highlights the non-degree-2 response (i.e., primarily  $l = 3$ ) (Figure 2b). For this calculation, the response at  $l = 3$  is several percent of that at  $l = 2$ , consistent with the results in Figure 1 for  $\Delta = 7.5\%$ . Figure 2b shows a localized negative (positive) response surrounded by a broad region of positive (negative) response on the nearside (farside). The nearside-farside patterns would reverse if  $V_s$  on the nearside is made faster than on the farside. It should be pointed out that actual tidal response pattern is more complicated than in Figure 2, because of the additional presence of the librational tide.

[14] The general form of the non-degree-2 response can be understood in terms of selection rules for products of

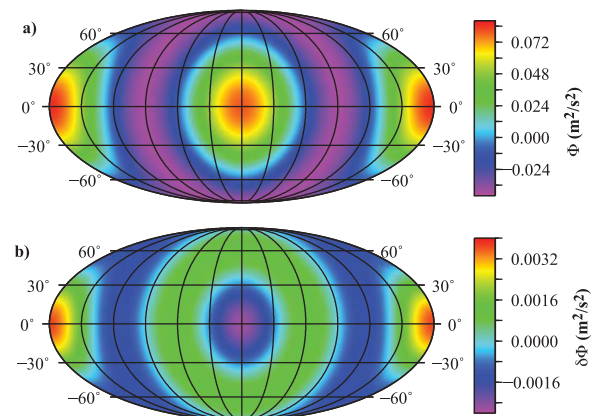


**Figure 2.** Maps of the response of the gravitational potential (a) for forcing caused by the radial tidal potential (i.e., the  $\cos(nt)$  term in (4)), with degree-1 structure variations where  $\Delta = 7.5\%$ , and the difference in the gravitational potential (b) between the case with  $\Delta = 7.5\%$  and a case with no lateral variations in elastic structure. Maps of the radial displacement and its difference between these two cases show similar patterns to Figures 2a and 2b, and are not plotted.

spherical harmonics [e.g., *Edmonds*, 1957]. Consider a laterally varying lunar structural feature, described by a harmonic  $(l, m)$ . Suppose the amplitude of this feature is small compared with the mean spherical structure. Then, to first order in this small perturbation, the response to  $(2, m_0)$  harmonic forcing will be dominated by that same  $(2, m_0)$  harmonic, but will also include small terms at degrees between  $2-l$  and  $2+l$ , and at orders  $m_0+m$ . Thus, for our degree 1 order 1 structure, the perturbation in the lunar gravitational potential induced by  $(2,0)$  forcing should include a  $(3,1)$  harmonic, and the perturbation induced by  $(2,2)$  forcing should include  $(3,3)$  and  $(3,1)$  harmonics. This is all consistent with the results shown in Figure 1. Note, incidentally, that the selection rules would normally imply a response at degree 1. However, degree-1 terms for the gravitational potential vanish in our center-of-mass coordinate system, while the degree-1 displacement response is about 2 orders of magnitude smaller than that at degree-3. Also note that there can be a significant response, though still smaller than that at degree-3, at other harmonics that are not predicted by the selection rules (e.g., at degree-4). This response is likely caused by non-linear mode-coupling for which the selection rules require higher-order perturbation analysis.

#### 4. Conclusion and Discussion

[15] For a lunar mantle with lateral variations in elastic structure, the mode-coupling leads to non-degree-2 gravitational and radial displacement signals in response to degree-2 tidal forcing. Our calculations show that if there is a 5% or larger degree-1 variation in seismic shear wave speed in the lunar mantle, the gravitational and radial displacement response at degree 3 ( $(3, 1)$  and  $(3, 3)$ ) may exceed 2% of the degree-2 response. The larger the degree-1 variations in mantle elastic structure, the greater the degree 3 response. We propose that observations of the non-degree-2 lunar tidal responses may help constrain the long-wavelength lunar mantle structure via lunar tidal tomography.

[16] The application of tidal tomography to constrain lunar mantle structure depends on two interconnected issues: 1) high precision observations of the non-degree-2 tidal response and 2) the amplitude of lateral variations in lunar mantle structure. Although point-measurements of lunar surface displacement at a small number of sites have been made since the Apollo mission via lunar laser ranging [e.g., *Williams et al.*, 2001], satellite measurements of the tidal gravitational response may be better suited for tidal tomography studies. Recent missions including Clementine [*Lemoine et al.*, 1997], Lunar Prospector [*Konopliv et al.*, 1998], and SELENE [*Namiki et al.*, 2009; *Matsumoto et al.*, 2010] have significantly improved models of the static lunar gravity field. The current GRAIL mission is designed to measure the lunar gravity field to unprecedented accuracy [*Zuber et al.*, 2012]. To perform tidal tomography studies such as those proposed here, the non-degree-2 tidal response must be extracted from the satellite data. The non-degree-2 tidal response, if caused by mode-coupling as discussed in this study, will have the same time dependence as the degree-2 tidal potential shown in (4) (i.e.,  $\cos(nt)$  for radial tidal forcing,  $\sin(nt)$  for librational tidal forcing), thus giving these terms a distinctive temporal signature.

[17] The form of the tidal potential shown in (4) is only an approximation. The exact expression includes spherical harmonics of all degrees. Thus, even for a spherically symmetric Moon, there will be tidal signals in the gravity field and surface displacements at degrees 3 and higher. It is natural to wonder whether those terms might degrade attempts to identify the effects of lateral inhomogeneities. Fortunately, this is not apt to be a serious problem. The amplitude of a degree  $l$  tidal potential term, is smaller than the degree-2 amplitudes by a factor of  $(\text{lunar radius/Earth-Moon distance})^{(l-2)}$  [e.g., *Agnew*, 2008, equation (4)]. That implies that the degree-3 forcing terms are smaller than the degree-2 terms by a factor of  $\sim 220$ . We find the value of the degree-3 Love number  $k_3$  is about 40% of the value of  $k_2$ , implying that the response of a spherically symmetric Moon to degree-3 tidal forcing is only about  $0.4/220$  or 0.2% of the response to degree-2 forcing. This is an order-of-magnitude smaller than the level of non-degree-2 response to degree-2 forcing described in this paper.

[18] However, the detectability of a non-degree-2 tidal response, i.e., its amplitude, depends on the amplitude of the lateral variations in lunar elastic structure (Figure 1). The possibility of using the tidal response to constrain Earth's mantle structure via tidal tomography was proposed by *Latychev et al.* [2009]. However, vigorous mantle convection for the Earth tends to diminish lateral variation, thus leading to reduced mode-coupling signals; although  $>10\%$  seismic velocity variations do exist in the continental lithosphere and near the core-mantle boundary, and are often attributed to compositional or partial melting effects [e.g., *Ritsema et al.*, 1999]. Lunar mantle convection was probably rather sluggish even in its early history, given the Moon's small size, which would help preserve laterally varying lunar mantle structure. Additionally, several lines of evidence suggest that the lunar mantle may be dominated by degree-1 structure of compositional origin [*Qin et al.*, 2012]. Therefore, it is possible that the lunar mantle has strong enough lateral variations in elastic structure to produce a detectable non-degree-2 tidal response. *Zhao et al.* [2008] reported  $\sim 2\%$  variations in Vs on the lunar nearside, using the Apollo seismic data. However, their seismic model did not give any information on the farside and hence on nearside-farside contrast as we propose here.

[19] We suggest that tidal observations from GRAIL and previous missions could provide significant constraints on lateral variations of the lunar interior structure that might improve understanding of the dynamical evolution of the lunar mantle and guide future lunar missions. Future studies should examine whether the non-degree-2 response to degree-2 tidal forcing can be extracted from GRAIL and other available observations, and can be used in our proposed lunar tidal tomography studies. Future studies should also determine the mode-coupling effects caused by other long-wavelength lunar mantle structures and by lateral variations in lunar mantle density, lame parameter  $\lambda$ , and crustal structure.

[20] **Acknowledgments.** The modifications of code CitcomSVE for compressible media were done by G. A. S. Z., and J. W., and will be described elsewhere. This work is supported by NASA PGG Program (grant NNX11AP59G).

[21] The Editor and authors thank Francis Nimmo and two other reviewers for assisting in the evaluation of this paper.

## References

- Agnew, D. C. (2008), Earth tides, in *Treatise on Geophysics*, vol. 3, *Geodesy*, edited by T. Herring and G. Schubert, pp. 163–195, Elsevier, Amsterdam.
- Dahlen, F. A., and J. Tromp (1998), *Theoretical Global Seismology*, 1025 pp., Princeton Univ. Press, Princeton, N. J.
- Edmonds, A. R. (1957), *Angular Momentum in Quantum Mechanics*, 146 pp., Princeton Univ. Press, Princeton, N. J.
- Frohlich, C., and Y. Nakamura (2009), The physical mechanism of deep moonquakes and intermediate-depth earthquakes: How similar and how different?, *Phys. Earth Planet. Inter.*, *173*, 365–374, doi:10.1016/j.pepi.2009.02.004.
- Garrick-Bethell, I., F. Nimmo, and M. A. Wieczorek (2010), Structure and formation of the lunar farside highlands, *Science*, *330*, 949–951, doi:10.1126/science.1193424.
- Kaula, W. M. (1964), Tidal dissipation by solid friction and the resulting orbital evolution, *Rev. Geophys.*, *2*, 661–685, doi:10.1029/RG002i004p00661.
- Konopliv, A. S., A. B. Binder, L. L. Hood, A. B. Kucinskas, and J. G. Williams (1998), Improved gravity field of the Moon from Lunar Prospector, *Science*, *281*, 1476–1480, doi:10.1126/science.281.5382.1476.
- Konopliv, A. S., S. W. Asmar, E. Carranza, W. L. Sjogren, and D. N. Yuan (2001), Recent gravity models as a result of the lunar prospector mission, *Icarus*, *150*, 1–18, doi:10.1006/icar.2000.6573.
- Lambek, K. (1980), *The Earth's Variable Rotation: Geophysical Causes and Consequences*, Cambridge Univ. Press, Cambridge, U. K., doi:10.1017/CBO9780511569579.
- Lammlein, D. R. (1977), Lunar seismicity and tectonics, *Phys. Earth Planet. Inter.*, *14*, 224–273, doi:10.1016/0031-9201(77)90175-3.
- Latychev, K., J. X. Mitrovica, M. Ishii, N.-H. Chan, and J. L. Davis (2009), Body tides on a 3-D elastic Earth: Toward a tidal tomography, *Earth Planet. Sci. Lett.*, *277*, 86–90, doi:10.1016/j.epsl.2008.10.008.
- Lawrence, D. J., W. C. Feldman, R. C. Elphic, R. C. Little, T. H. Prettyman, S. Maurice, P. G. Lucey, and A. B. Binder (2002), Iron abundances on the lunar surface as measured by the Lunar Prospector gamma-ray and neutron spectrometers, *J. Geophys. Res.*, *107*(E12), 5130, doi:10.1029/2001JE001530.
- Lemoine, F. G., D. E. Smith, M. T. Zuber, G. A. Neumann, and D. D. Rowlands (1997), A 70th degree lunar gravity model (GLGM-2) from Clementine and other tracking data, *J. Geophys. Res.*, *102*, 16,339–16,359, doi:10.1029/97JE01418.
- Matsumoto, K., et al. (2010), An improved lunar gravity field model from SELENE and historical tracking data: Revealing the farside gravity features, *J. Geophys. Res.*, *115*, E06007, doi:10.1029/2009JE003499.
- Nakamura, Y. (2005), Farside deep moonquakes and deep interior of the Moon, *J. Geophys. Res.*, *110*, E01001, doi:10.1029/2004JE002332.
- Namiki, N., et al. (2009), Far side gravity field of the Moon from four-way Doppler measurements of SELENE (Kaguya), *Science*, *323*, 900–905, doi:10.1126/science.1168029.
- Neumann, G. A., M. T. Zuber, D. E. Smith, and F. G. Lemoine (1996), The lunar crust: Global structure and signature of major basins, *J. Geophys. Res.*, *101*, 16,841–16,843, doi:10.1029/96JE01246.
- Parmentier, E. M., S. J. Zhong, and M. T. Zuber (2002), Gravitational differentiation due to initial chemical stratification: Origin of lunar asymmetry by the creep of dense KREEP, *Earth Planet. Sci. Lett.*, *201*, 473–480, doi:10.1016/S0012-821X(02)00726-4.
- Paulson, A., S. J. Zhong, and J. Wahr (2005), Modelling post-glacial rebound with lateral viscosity variations, *Geophys. J. Int.*, *163*(1), 357–371, doi:10.1111/j.1365-246X.2005.02645.x.
- Qin, C., A. Muirhead, and S. J. Zhong (2012), Correlation of deep moonquakes and mare basalts: Implications for lunar mantle structure and evolution, *Icarus*, *220*, 100–105.
- Ritsema, J., J. van Heijst, and J. H. Woodhouse (1999), Complex shear wave velocity structure imaged beneath Africa and Iceland, *Science*, *286*, 1925–1928, doi:10.1126/science.286.5446.1925.
- Tobie, G., A. Mocquet, and C. Sotin (2005), Tidal dissipation within large icy satellites: Applications to Europa and Titan, *Icarus*, *177*, 534–549, doi:10.1016/j.icarus.2005.04.006.
- Wahr, J., et al. (2009), Modeling stresses on satellites due to nonsynchronous rotation and orbital eccentricity using gravitational potential theory, *Icarus*, *200*, 188–206, doi:10.1016/j.icarus.2008.11.002.
- Weber, R. C., P. Y. Lin, E. J. Garnero, Q. Williams, and P. Lognonne (2011), Seismic detection of the lunar core, *Science*, *331*, 309–312, doi:10.1126/science.1199375.
- Wieczorek, M. A., and R. J. Phillips (2000), The Procellarum KREEP Terrane: Implications for mare volcanism and lunar evolution, *J. Geophys. Res.*, *105*(E8), 20,417–20,430, doi:10.1029/1999JE001092.
- Wieczorek, M. A., et al. (2006), The constitution and structure of the lunar interior, in *New Views of the Moon*, *Rev. Mineral. Geochem.*, vol. 60, edited by D. J. Vaughan, pp. 221–364, Mineral. Soc. of Am., Chantilly, Va., doi:10.2138/rmg.2006.60.3.
- Williams, J. G., D. H. Boggs, C. F. Yoder, J. T. Ratcliff, and J. O. Dickey (2001), Lunar rotational dissipation in solid body and molten core, *J. Geophys. Res.*, *106*, 27,933–27,968, doi:10.1029/2000JE001396.
- Zhao, D., J. Lei, and L. Liu (2008), Seismic tomography of the Moon, *Chin. Sci. Bull.*, *53*, 3897–3907, doi:10.1007/s11434-008-0484-1.
- Zhong, S. J., E. M. Parmentier, and M. T. Zuber (2000), A dynamic origin for the global asymmetry of lunar mare basalts, *Earth Planet. Sci. Lett.*, *177*, 131–140, doi:10.1016/S0012-821X(00)00041-8.
- Zhong, S. J., A. Paulson, and J. Wahr (2003), Three-dimensional finite-element modelling of Earth's viscoelastic deformation: Effects of lateral variations in lithospheric thickness, *Geophys. J. Int.*, *155*(2), 679–695, doi:10.1046/j.1365-246X.2003.02084.x.
- Zhong, S. J., A. K. McNamara, E. Tan, L. Moresi, and M. Gurnis (2008), A benchmark study on mantle convection in a 3-D spherical shell using CitcomS, *Geochem. Geophys. Geosyst.*, *9*, Q10017, doi:10.1029/2008GC002048.
- Zuber, M. T., D. E. Smith, F. G. Lemoine, and G. A. Neumann (1994), The shape and internal structure of the Moon from the Clementine mission, *Science*, *266*, 1839–1843, doi:10.1126/science.266.5192.1839.
- Zuber, M. T., et al. (2012), Gravity recovery and interior laboratory (GRAIL) mission: Status at the initiation of the science mapping phase, *Lunar Planet. Sci. Conf.*, *43rd*, Abstract 1489.